Accepted Manuscript

Establishment of a 3D-dynamic osteoblasts–osteoclasts co-culture model to simulate the jawbone microenvironment *in vitro*

Letizia Penolazzi, Andrea Lolli, Luca Sardelli, Marco Angelozzi, Elisabetta Lambertini, Leonardo Trombelli, Francesca Ciarpella, RenataVecchiatini, Roberta Piva

Please cite this article as: Penolazzi Letizia, Lolli Andrea, Sardelli Luca, Angelozzi Marco, Lambertini Elisabetta, Trombelli Leonardo, Ciarpella Francesca, RenataVecchiatini, Piva Roberta, Establishment of a 3D-dynamic osteoblasts–osteoclasts co-culture model to simulate the jawbone microenvironment *in vitro*, *Life Sciences* (2016), doi: 10.1016/j.lfs.2016.03.035

Establishment of a 3D-dynamic osteoblasts-osteoclasts
co-culture model to simulate the jawbone microenvironment *in vitro*

Letizia Penolazzi, Andrea Lolli, Luca Sardelli, Marco Angelozzi, Elisabetta Lambertini, Leonardo Trombelli, Francesca Ciarpella, RenataVecchiatini, Roberta Piva*

Department of Biomedical and Specialty Surgical Sciences, University of Ferrara

* Corresponding author at:
Department of Biomedical and Specialty Surgical Sciences, University of Ferrara,
Via Fossato di Mortara, 74 - 44121, Ferrara, Italy.
Tel.: +39 0532974405; fax: +39 0532974405.
E-mail address: piv@unife.it

1

ABSTRACT

Aims: We aimed to establish a 3D osteoblasts/osteoclasts co-culture system requiring limited amounts of human primary cells and useful as platform to 1. recapitulate an "oral bone microenvironment" in healthy or pathological condition, and 2. produce potential implantable cell constructs for regeneration of jawbone which can be negatively affected by bisphosphonates (BPs).

Main methods: Osteoblasts from normal bone chips (hOBs) or from jawbone of patients taking BPs (hnOBs) were co-cultured with monocytes (hMCs) either in static (3D-C) or dynamic (3D-DyC) condition using the RCCS-4™ bioreactor for 3 weeks. Cell aggregates were characterized for viability, histological features and specific osteoclastic and osteogenic markers.

Key findings: In all tested conditions hOBs supported the formation of mature osteoclasts (hOCs), without differentiating agents or exogenous scaffolds. 3D-DyC condition associated with a ground based condition (Xg) rather than modeled microgravity (μXg) produced aggregates with high level of osteogenic markers including Osteopontin (OPN), Osterix (OSX), Runx2 and appreciable bone mineral matrix. hnOBs co-cultured with hMCs in 3D-Dyc/Xg condition generated OPN and mineral matrix positive aggregates.

Significance: We optimized a 3D co-culture system with a limited amount of cells preserving viability and functionality of bone cellular components and generating bone-like aggregates also by using cells from jawbone necrotic tissue. The feasibility to obtain from poor-quality bone sites viable osteoblasts able to form aggregates when co-cultured with hMCs, allows to study the development of autologous implantable constructs to overcome jawbone deficiency in patients affected by MRONJ (Medication-Related Osteonecrosis of the Jaws).

Keywords: 3D cell co-culture, MRONJ, osteoblasts, osteoclasts

1. Introduction

Three-dimensional co-culture systems have been developed greatly within the last decade in an effort to recreate the physiological cellular microenvironment of a specific tissue, and extend cell culture longevity and functionality [18,19, 32].

Regarding bone tissue, several *in vitro* co-culture systems based on bone-forming cells (osteoblasts, OBs)/bone-resorbing cells (osteoclasts, OCs) have been proposed [5, 9, 14, 17, 20, 37], with the aim of creating the Basic Multicellular Unit (BMU). Different parameters such as cell sources and culture conditions may influence the establishment of the complex interactions and intimate crosstalk that naturally occur *in vivo* between OBs, OCs and their precursors [33, 35, 26, 11]. In an effort to make the results of these studies the most informative and reproducible, the majority of the evidence were so far obtained using a substantial number of cells that could guarantee the formation of an appreciable cellular aggregate. For this reason cell lines, such as MC3T3-E1, MG63 and SaOS-2 for the osteoblastic lineage, and RAW264.7 for the osteoclast lineage are widely used. However, cell lines often fail mimicking the primary counterparts. Considering osteoclastic lineage, peripheral blood mononuclear cells (PBMCs), bone marrow and spleen-derived cell populations are good precursors for adequate amount of primary OCs [38,16]. Setting up abundant primary cultures of OBs from human tissues is more challenging. In many cases a limited number of precursors or mature cells from a given source can be obtained with a noninvasive procedure and, consequently, few cells are available for *in vitro* or *in vivo* experiments. This occurs when the cells are harvested from atrophic tissue, with insufficient bone quality and volume, or in sites lacking of stem and progenitor cells due to extensive trauma, radiation therapy, or medications such as bisphosphonates (BPs) antiresorptive drugs. BPs promote proliferation and differentiation of OBs and inhibit OCs [28]. Sometimes these conditions hesitate in adverse non-healing lesions, such as Medication-Related Osteonecrosis of the Jaws (MRONJ), a condition of exposed bone in the maxillofacial region compromising the quality of life with significant morbility [30, 29]. The optimal treatment strategy for MRONJ is still to be established. BPs treatment cessation is not sufficient to restore reparative process, conversely, targeted interventions of regenerative medicine could be an attractive option [6, 15, 1, 10]. In this context, the replacement of healthy bone in necrotic lesions represents an important bone tissue engineering challenge [8, 4].

These considerations led us to study the minimal combination of OBs/OCs able to promote cell aggregation and differentiation mimicking a bone microenvironment in a 3D static or dynamic co-culture system. Different culture conditions with limited amount of human primary bone cells in a perfusion bioreactor [36, 7] have been explored in order to set up a protocol exportable to critical

3

situations. Specifically, the possibility to obtain vital bone specimens from jaw bone of patients taking BPs was evaluated, in order to investigate the potential of cells from such a compromised tissue area, assuming that the approach here described could be helpful to generate an autologous implantable construct.

2. Materials and methods

2.1. Cell culture and harvesting procedure

Human normal osteoblasts (hOBs) were obtained from nasal septum. Bone fragments from nasal septum [34] ere obtained from healthy donors between 25-60 years old undergoing septoplasty surgery procedures after informed consent and approval of the Ethics Committee of the University of Ferrara and S. Anna Hospital. Briefly, bone chips were dissected into smaller pieces and plated in T-25 culture flasks in 50% DMEM high-glucose / 50% DMEM F-12 / 20% Fetal Calf Serum (FCS) (Euroclone S.p.A., Milan, Italy) supplemented with 1 mM L-Glutamine, antibiotics (penicillin 100 μg/mL and streptomycin 10 μg/mL) at 37 °C in a humidified atmosphere of 5% CO_2. At 70–80% of confluence, cells were scraped off by treatment with 0.05 % trypsin-ethylenediaminetetraaceticacid (EDTA) (Sigma-Aldrich, St. Louis, MO, USA), washed, plated and allowed to proliferate in standard conditions (10% FCS DMEM high-glucose). hOBs (p0) were characterized for the presence of alkaline phosphatase activity (ALP Leukocyte kit; Sigma-Aldrich). Osteopontin (OPN) and RUNT-related transcription factor 2 (Runx2) expression was assessed by immunostaining. For osteogenic differentiation, hOBs were cultured up to 21 days in osteogenic medium consisting of 10% FCS DMEM high-glucose supplemented with 10 mM β-glycerophosphate, 10^{-7} M dexamethasone and 100 μM ascorbate (Sigma-Aldrich). The osteogenic medium was refreshed twice a week and the extent of mineralized matrix in the plates was determined by Alizarin Red S staining (ARS; Sigma-Aldrich). For co-culture experiments hOBs were used until passage 3.

Human osteoblasts from jawbone of patients taking BPs at risk for "necrotic" lesions (hnOBs) were obtained as described below. Harvesting procedures of autogenous bone were conducted in full accordance with the "Declaration of Helsinki" as adopted by the 18th World Medical Assembly in 1964 and revised in Edinburgh (2000) and the Good Clinical Practice guidelines. Before surgery, each subject provided an informed consent. All surgical extractions and treatments were performed by the same clinician, according to standard surgical and anaesthetic protocols of University Dental Clinic, University of Ferrara.

Bone specimens were harvested from alveolar process during surgical planned treatments in different patients:

- patients previously treated with antiresorptive agents, such as Zoledronate or Alendronate, for metastatic disease or osteoporosis, undergoing to routinary tooth extraction;

5

- patients previously treated with antiresorptive agents, such as Zoledronate or Alendronate, for metastatic disease or osteoporosis, undergoing to surgical treatment of MRONJ.

There was no history of radiation therapy to the head and neck region in any of these patients.

Before surgical treatment mepivacaine 3% was locally administered, as needed. Buccal flaps were raised, lingual tissues were retracted and protected. After tooth extraction, buccal and distal alveolar bone was harvested with bone scraper (Safescraper® Twist Cortical Bone Collector, Meta, Italy).

Considering the risk for MRONJ onset, each patient received same standard preoperative therapy (amoxicillin 1gr 2 times a day starting 3 days before surgery; metronidazole 250 mg 3 times a day starting 3 days before surgery) and postoperative instructions for Nonsteroidal anti-inflammatory drugs (NSAIDs) and antibiotics prescription (amoxicillin 1gr 2 times a day for 10 days; ketoprofen 80 mg 3 times a day for day 1, 2 and 3). Chlorhexidine 0.20% mouthrinses were prescribed from day 2 until day 14. A post-operative meeting was scheduled for day 7 and day 10, to check swelling and primary wound closure. During the second meeting sutures were removed.

During surgical treatment of MRONJ, bone specimen were collected with the use of a Modified Trephine Bur n. TRE040M (Hu-Friedy Mfg. Co., LLC).

As proposed by Cardemil et al. [6], the alveolar bone samples were collected some distance away from exposed necrotic bone (Fig. 6A), within the considered boundary bone. The boundary of the MRONJ lesion was defined where vital, light, and bleeding jawbone replaced grayish, brittle, and necrotic bone [6].

Considering the presence of MRONJ, each patient received same standard preoperative therapy (amoxicillin 1gr twice a day starting 6 days before surgery; metronidazole 250 mg 3 times a day starting 3 days before surgery) and postoperative instructions for Nonsteroidal anti-inflammatory drugs (NSAIDs) and antibiotics prescription (amoxicillin 1gr twice a day for 10 days; metronidazole 250 mg 3 times a day for 10 days; ketoprofen 80 mg 3 times a day for day 1, 2 and 3. Chlorhexidine 0.20% mouthrinses were prescribed from day 2 until day 14. A post-operative meeting was scheduled for day 7 and day 10, to check swelling and primary wound closure. During the second meeting sutures were removed.

After specimens collections, in all cases surgical area was treated with piezo-electric surgery, and it was cleaned with either a diamond (piezo) or a round diamond-burr drill, at low speed and with generous saline irrigation, leaving dense, highly mineralized bone. Finally the wound space was thoroughly debrided then closed with interrupted sutures (Vicryl 4-0, Ethicon Spa, Pomezia, Italy), to achieve a primary closure, as appropriate.

6

The samples were dissected into smaller pieces, plated and cultured in T-25 culture flasks as already described. The culture medium for hnOBs was further supplemented with a 5-fold increased concentration of antibiotics (penicillin 500 μg/mL and streptomycin 50 μg/mL, gentamicin 50 μg/mL) and antimycotic (fungizone 10 μg/mL): we adopted these conditions given the derivation of the samples and the consequent possibility of contaminations. hnOBs were characterized by immunocytochemical analysis for OPN and Runx2 and ARS staining after osteogenic induction, as already described.

Human monocytes (hMCs) were obtained from peripheral blood (PB) of healthy volunteers (different from the donors of hOBs) after informed consent (median age 37.5 years, range 25-50 that is approximately the same age range of the hOBs donors). PB mononuclear cells (PBMCs) were obtained from diluted peripheral blood (1:2 in Hanks solution), separated by Histopaque$^{®}$-1077 (Sigma-Aldrich). hMCs were purified from PBMCs by adhesion selection on polystyrene plates: $1x10^6$ PBMCs/cm^2 were plated in T-25 culture flasks, allowed to settle for 4 hours at 37° and flasks were then rinsed to remove non-adherent cells (lymphocytes, platelets, red blood cells, polymorphonuclear cells) [27]. The purity of hMCs population was verified by cytofluorimetric analysis. Briefly, $1x10^5$ cells were resuspended in phosphate-buffered saline (PBS) and incubated with fluorescein isothiocyanate (FITC) conjugated anti-human CD14 antibody (ImmunoTools GmbH, Friesoythe, Germany) for 15 min at 4°C. A monoclonal antibody with no specificity was used as negative control. Cells were then washed and resuspended in 400 μL of PBS. The fluorescence levels were measured using the FACS Scan flow cytometer (Becton Dickinson, Franklin Lakes, NJ, USA) and CELLQUEST software (Becton Dickinson European HQ, Erembodegem Aalst, Belgium). Only the samples that after FACS analysis were CD14 positive ≥95% were used. In order to confirm the ability of isolated hMCs to differentiate into mature osteoclasts (hOCs), M-CSF (25 ng/mL) and RANKL (30 ng/mL) (PeproTech EC Ltd, London, UK) were added to the culture medium. After 7-10 days, TRAP staining [27] was carried out with the Acid Phosphatase Leukocyte (TRAP) Kit no. 386 (Sigma-Aldrich) according to the manufacturer's protocol. The expression levels of the osteoclast-specific markers MMP-9 and Cathepsin K were assessed by immunocytochemistry.

Furthermore in order to verify their resorbing ability, hMCs were plated into a calcium phosphate-coated OAAS (OAAS, Osteoclast Activity Assay Substrate, Oscotect Inc., Seoul, Korea) at the density of $1x10^6$ cells/well, and maintained in the same culture condition indicated above. After 7 days, when TRAP-positive hOCs appeared, the cells were

7

removed with a solution of 5% sodium hypochlorite. Bone resorption activity was measured by direct observation under phase contrast microscopy.

2.2. Indirect hOBs/hOCs co-culture system

$1,5x10^5$ hOBs were pre-cultured on polystyrene 24 well plates until confluence, then 0.45 μm Cell Culture Inserts (Becton Dickinson, NJ, USA) seeded with hMCs ($0,5x10^5$, hOBs/hMCs 3:1 cell ratio) were added. Cells were cultured in 10% FCS DMEM high-glucose in the absence of osteoclastogenic inducers (MCSF and RANKL). This method established a co-culture condition with the two cell types not coming into contact, but allowing the interaction with the soluble factors produced by the cells. Co-cultures exposed to M-CSF (25 ng/mL) and RANKL (30 ng/mL) were used as positive control, while hMCs cultured in the absence of hOBs were employed as negative control. After 7 days, TRAP staining and immunocytochemistry analysis for Cathepsin K were carried out on cells cultured in the upper chamber in order to verify the presence of mature osteoclasts (hOCs). After 14 day of osteogenic induction, the expression levels of OPN, OSX and Runx2, the ALP activity and the presence of mineralized matrix deposition (ARS staining) were analyzed.

Each individual experiment was entirely performed with hMCs from PBMCs from the same identical donor.

2.3. hOBs/hOCs three-dimensional co-culture systems

hOBs/hOCs aggregates were generated in the absence of exogenous scaffolds by using two different experimental approaches: 3D co-culture system obtained in static condition (*3D-C*) and in dynamic condition (*3D-Dyc*).

For *3D-C* culture condition, $0.5-1x10^6$ hMCs were incubated with $1-2x10^6$ hOBs in agarose coated polystyrene 6 well plate, in 2 mL of 10% FCS DMEM high-glucose at 37°C (humidified atmosphere, 5% CO_2), with the medium being changed twice a week. After 24h, the presence of spheroids with a diameter >500μm was observed. After 7 days, a first set of aggregates were collected, fixed in 4% formalin, embedded in paraffin, sectioned and processed for TRAP analysis. *3D-C* aggregates were maintained in osteogenic medium (see above) for further 14 days of co-culture. The aggregates were then fixed, embedded in paraffin, sectioned and processed for histochemisty.

The 3D dynamic culture (*3D-DyC*) condition was set up by using the RCCS-4TM bioreactor (Synthecon™, Inc., Houston, TX, USA), with a High Aspect Ratio Vessel (HARV[TM]; Synthecon™, Inc., Houston, TX, USA). The HARV vessel consists of a horizontally rotated culture chamber, where the cells are suspended, and a perfusion system with media continuously flowing through the culture chamber. The culture chamber can rotate in the X-axis at certain speeds (rpm): higher rpm are associated to lower gravity. $0.5-1x10^6$ hMCs and $1-2x10^6$ hOBs were inoculated in 2 mL HARV vessels filled with 10% FCS DMEM high-glucose and all air bubbles were removed from the culture chamber. HARV vessels were then inserted into the RCCS-4TM rotary bioreactor and placed in an incubator at 37°C, for the indicated times, in a humidified atmosphere with 5% CO_2. After 7 days, a first set of aggregates were collected for TRAP assay and the others were maintained for further 14 days in osteogenic medium. The rotation speed used for the bioreactor was 4 rpm for the Ground Based dynamic culture at 1xg (Xg) and 14-16 rpm for the Modeled Microgravity condition (μXg), where the aggregate floated in suspension. Medium was refreshed twice a week. At the end-point of co-culture (21 days), the aggregates were collected, 4% formalin fixed and embedded in paraffin for further analysis. All the tested experimental conditions are reported in Fig. 3.

The hnOBs/hMCs aggregate was obtained after incubation of $0.5x10^6$ hMCs and $1x10^6$ hnOBs, inoculated in 2 mL HARV vessel, inserted into the RCCS-4TM rotary bioreactor (37°C, humidified atmosphere, 5% CO_2), cultured in the absence of modeled microgravity (3DyC/Xg condition) and collected after 21 days (of which 14 days in osteogenic medium) for viability and histological analysis.

2.4. Cell viability

Viability of the cells was analyzed by double staining with propidium iodide and Calcein-AM assay (Sigma-Aldrich), according to the manufacturer's instructions. Cells were observed under a fluorescence microscope (Nikon, Optiphot-2; Nikon Corporation, Tokyo, Japan) using the filter block for fluorescein. Dead cells were stained in red, whereas viable ones appeared in green.

2.5. Immunocytochemistry and histology

Immunocytochemistry analysis was performed employing the ImmPRESS (Vectorlabs, Burlingame, CA) or 4plus AP universal (Biocare Medical, Concord, CA) detection kit. Briefly, cells grown in 12-wells plate or from indirect co-culture were fixed in cold 100% methanol and permeabilized with 0.2% (v/v) Triton X-100 (Sigma-Aldrich) in TBS (Tris-buffered saline). Cells

9

were treated with 3 % H_2O_2 in TBS 1x and incubated in 2 % normal horse serum (Vectorlabs, Burlingame, CA) for 15 min at room temperature. After the incubation in blocking serum, the different primary antibodies were added and incubated at 4 °C overnight: polyclonal antibodies for MMP-9 (H-129), OPN (LF-123), Runx2 (M-70), OSX (M-15), Cathepsin K (E-7) (rabbit anti-human, 1:200 dilution, Santa Cruz Biotechnology, Dallas TX USA). Cells were then incubated in Vecstain ABC (Vectorlabs, Burlingame, CA) or Universal AP detection (Biocare Medical, Concord, CA) reagents for 30 minutes and stained, respectively, with DAB solution (Vectorlabs, Burlingame, CA) or Vulcan Fast Red chromogen kit (Biocare Medical, Concord, CA). After washing, cells were mounted in glycerol and observed using the Nikon Esclipse 50i optical microscope.

Histological sections (5 μm) of *3D-C* and *3D-Dyc* aggregates were subjected to immunohistochemistry. To this aim, non-consecutive sections were immunostained with a primary antibody against Cathepsin K (E-7), OPN (LF-123), OSX (M-15), Runx2 (M-70) (rabbit anti-human, 1:100 dilution, Santa Cruz biotec.). Histological sections were deparaffinized, rehydrated and enzymatic treated with 1 mg/mL pronase and 10 mg/ml hyaluronidase (Sigma-Aldrich) for antigen retrieval and permeabilization. Slides were then incubated overnight with the primary antibody in a humid chamber at 4°C. Alkaline phosphatase-labeled secondary antibody was used (4plus Universal AP Detection, Biocare Medical, Concord, CA, USA) in combination with the Vulcan Fast Red Chromogen Kit (Biocare Medical, Concord, CA, USA), resulting in a red staining. The sections were counterstained with hematoxylin, mounted in glycerol and observed using the Nikon Esclipse 50i optical microscope. TRAP staining was carried out with the Acid Phosphatase Leukocyte (TRAP) Kit no. 386 (Sigma-Aldrich) according to the manufacturer's protocol as already reported [28]. For Alizarin Red S staining, cells cultured in monolayer or 3D aggregates (*3D-C* and *3D-Dyc*) were fixed in 4% formalin, and then stained with 40 mM Alizarin Red S solution (pH 4.2) at room temperature for 10 min. Samples were rinsed five times with distilled water and washed three times in PBS on an orbital shaker at 40 rpm for 5 min each, to reduce non-specific binding.

The stainings were quantified by a computerised video camera-based image analysis system (NIH, USA ImageJ software, public domain available at: http://rsb.info.nih.gov/nih-image/) under brightfield microscopy (Nikon Eclipse 50i; Nikon Corporation, Tokyo, Japan). For the analysis of sections obtained from *3D-C* and *3D-Dyc* aggregates, the positive immunostaining was expressed as % of positive area (three replicates per donors were acquired; five sections per sample; n = 3).

2.6. Statistical analysis

10

Statistical significance was analysed by one-way analysis of variance (ANOVA) and Bonferroni post hoc test if the values followed a normal distribution, or by Kruskal–Wallis analysis (nonparametric one-way ANOVA) and Dunn's post hoc test if the values were not normally distributed. For all statistical analysis, differences were considered statistically significant for p-values ≤ 0.05.

3. Results

3.1. Phenotypical characterization of hOBs and hOCs monotype cell cultures.

hOBs were characterized for their osteogenic potential, in terms of alkaline phosphatase activity (ALP), OPN and Runx2 expression and deposition of mineral matrix after 21 days of culture (Fig. 1A). Monocytes (hMCs) from human peripheral blood were used as osteoclast progenitors source. hMCs purification by adhesion selection on polystyrene plates (4 h, 37°C) allows to remove contaminating blood cells (lymphocytes, platelets, red blood cells, polymorphonuclear cells), as confirmed by microscopic observations and flow cytometric characterization. As shown in Fig. 1B we obtained more than 95% of purified hMCs, as calculated on the basis of forward and side light scatter profiles and cell surface display pattern (CD14). The ability of the purified hMCs to differentiate into mature multinucleated osteoclasts (hOCs) after exposure to osteoclastogenic inducers (MCSF and RANKL) was tested, by evaluating the positivity for the tartrate resistant acid phosphatase (TRAP), immunostaining for the osteoclast-specific matrix metalloproteinase-9 (MMP-9) and Cathepsin K, and the pit formation ability.

3.2. Indirect hOBs/hOCs co-culture system

An indirect hOBs/hMCs co-culture system was used to validate the differentiation potential of our experimental model to be used in subsequent three-dimensional (3D) co-culture systems. The ability of hOBs to support osteoclastogenesis was investigated seeding hMCs on polystyrene culture plate inserts in the simultaneous presence of hOBs (lower chamber) and without any osteoclastogenic inducers. We found that 1:3 hMCs/hOBs ratio was the optimal seeding condition allowing the induction of a high percentage of mature TRAP and Cathepsin K positive

11

multinucleated osteoclasts (hOCs) already detectable after 7 days of culture (Fig. 2, panels a,b,g). The hOCs formation observed in these conditions was comparable with that found when osteoclastogenic inducers were added in the medium (Fig. 2, panels c,d,h). On the contrary, when hOBs were omitted no hOCs were generated (Fig. 2, panels e,f,i). With the progression of culture in osteogenic medium the expression of OPN, OSX, Runx2, the ALP activity and the deposition of mineralized matrix were observed at day 21, indicating that the conventional 2D indirect co-culture system also supported osteoblast maturation.

3.3. hOBs/hOCs three-dimensional co-culture systems

Two different types of 3D environments were then used comparing the effect of static culture (*3D-C*) and dynamic flow (*3D-DyC*) conditions on co-culture systems (Fig. 3A). *3D-C* condition was obtained by direct combination of hMCs and hOBs in agarose coated polystyrene wells, while *3D-DyC* by growing the same cells in the horizontally rotated culture chamber High Aspect Ratio Vessels (HARV) applied to the Rotary Cell Culture System (RCCS). In *3D-DyC* the cells were maintained up to 21 days in controlled microgravity condition - Modeled Microgravity (µXg) - where the aggregate floated in suspension (14-16 rpm), or in 1x g condition - Ground Based dynamic culture (Xg) - where the aggregate was in continuous falling rotation close to the bottom of the vessel (4 rpm).

To valuate the optimal condition to generate spontaneously cellular aggregates, the tests reported in the insert of Fig. 3A have been performed. These included the variation of i. cell number and ratio; ii. exposure to differentiating agents (MCSF and RANKL); iii. rotation rate and modeled microgravity; and iiii. days in culture. Despite it is difficult to characterize the aggregation process, microscopic observations revealed an initial formation of cell assemblies that over time formed spherical aggregates both in *3D-C* and *3D-DyC* condition, mostly when $3x10^6$ cells/mL was used. Cell ratio had no effect for *3D-C*, but appeared relevant for *3D-DyC* condition where cell aggregation process is favored by 1:2 hMCs/hOBs ratio. The presence of inducers (MCSF/RANKL) was negligible to osteoclastogenic process. Interestingly, already after 7 days of culture, *3D-DyC* condition supported the formation of a functional aggregate exhibiting TRAP positivity (Fig. 3B). Together these findings suggest that all tested environments are favorable to aggregate formation.

3.4. Functionality of the cells within 3D-C and 3D-DyC aggregates

Considering that the overall function of the aggregate depends on the architecture that it achieved in

12

culture, the next experiments were performed at day 21 of culture after allowing the cells to better organize within the aggregate. Before processing for histological analysis, aggregates were subjected to Calcein AM/Propidium iodide (PI) double staining for cell viability assessment. As shown in Fig. 4, both *3D-C* and *3D-DyC* conditions generated aggregates that appeared highly viable at comparable level. Evidently, more than 95% of the cells were viable and remained intact within the aggregate up to day 21 of culture. Interestingly, haematoxylin staining of histological sections revealed appreciable different organization. In both conditions, after 21 days of culture the mass appeared more compact when compared with the cellular aggregate at day 7. This suggests that intercellular crosstalk, cell-stroma interactions and arrangements of the cells change over time, promoting the formation of a cell aggregate progressively better organized. However, in comparison with *3D-DyC*, cells within aggregates from *3D-C* appeared poorly organized. In fact, *3D-DyC* aggregates displayed a layered structure with an appreciable cellular organization: an outer region (arrows) surrounding the aggregate, an intermediate region with a trabecular-like structure and an inner region with different morphological characteristics (Fig. 4).

The functional properties of the cells within the aggregates were then investigated. As shown in Fig. 5 A, *3D-C* and *3D-DyC* conditions revealed substantial TRAP and Cathepsin K positivity demonstrating the presence of functional osteoclasts in the aggregates. For what concerns the osteoblastic cellular component (Fig. 5 B), *3D-C* aggregates clearly exhibited a low expression of OPN, OSX and Runx2 and a faint ARS staining compared to *3D-DyC* aggregates. Detailed analysis of *3D-DyC* conditions revealed that functionality of the hOBs grown in Xg seems to be better that those maintained in μXg. Xg condition induced a more solid cellular organization with numerous osteogenic markers positive areas than found in *3D-DyC* aggregates subjected to Modeled Microgravity.

The presence of the hMCs in the culture is critical to the formation of a functional aggregate. In fact, a 3D-monoculture of hOBs alone failed to organize in a well defined cellular aggregate as well as to deposit mineral matrix even in the most favorable condition (*3D-DyC Xg)* (Supplemental Fig. 1).

3.5. Human primary osteoblasts from jawbone of patients taking BPs with or without MRONJ lesion (hnOBs)

After demonstrating the feasibility to produce a construct mimicking the bone microenvironment from a small number of cells, we investigated the possibility to apply the same approach with cells from anatomic critical conditions.

13

In a first step, we investigated if a suitable, although low, number of osteoblasts could be obtained from jawbone of patients taking BPs (hnOBs). Bone chips were collected from 6 patients undergoing oral surgery for different reasons (see Table 1 for clinical parameters).

Considering donors, they were all female subjects, as reflection of higher prevalence of BPs prescription in the female population as consequence of indications to BPs treatment for specific underling diseases (i.e. osteoporosis, breast cancer, multiple myeloma) [30]. Recently co-morbid conditions among cancer patients were inconsistently reported to be associated with an increased risk for MRONJ, include anemia and diabetes [30].

Considering anatomic factors, all samples were harvested from mandible, while one sample was harvested during MRONJ surgical treatment. Nowadays limited new information regarding anatomic risk factors for MRONJ is available [30]. MRONJ is more likely to appear in the mandible (73%) than the maxilla (22.5%) but can appear in both jaws (4.5%) [30].

Once harvested, bone chips were maintained in basal medium condition without adding growth factors for the time required (thirty days at least) so that the cells spread out and grow as small clusters until confluence is reached. We observed that these cells required a higher expansion time than hOBs. One out of six samples failed to give cells in culture. From the other five samples the cells spread out, attached to the plastic surface and assumed a spindle-shape morphology. However, due to the peculiarity of the source, two samples encountered bacterial contamination, while another has not proliferated. Therefore, positive outcomes have been obtained from two samples (sample n. 5 and sample n. 6) which gave rise to proliferating and viable cells. These cells were recognizable as hnOBs since retained high OPN and Runx2 expression levels, as revealed by immunocytochemical analysis after (Fig. 6A). Furthermore, the positive staining for extracellular calcium deposition at day 21 of culture in osteogenic medium demonstrated the functional ability of hnOBs to deposit mineral matrix.

Despite the limitations related to the number and quality of the cells, we tried to combine these hnOBs from sample n. 5 and sample n. 6 with hMCs in the most favorable condition represented by *3D-DyC* in Xg. An appreciable aggregate consisting of viable cells were formed in both cases (Fig. 6B). Therefore, despite starting from hnOBs of poor quality, these cells were able to interact with hMCs contributing to give rise to a substantial aggregate characterized by TRAP positive areas associated with osteoblasts expressing OPN and producing Alizarin Red stained small noduli.

4. Discussion

To date, several *in vitro* experimental models have been proposed for basic research aimed to investigate bone diseases and bone repair. A great opportunity comes from 3D co-culture systems of different cells in combination with natural or synthetic scaffolds, generating cell-based constructs that potentially resemble the bone microenvironment *in vitro* [13, 12]. To be easily handled and well characterized cell aggregates need to be formed by a substantial number of cells, and, for these reasons, most of the evidence from literature refers to human or murine cell lines [25, 21]. As a consequence, while this approach may be useful to standardize and optimize culture conditions, it is hardly exportable to human primary cells. On the other hand, the use of cells obtained from the patient is an essential step towards a better elucidation of the pathogenetic mechanisms and the development of novel treatments inspired by the principle of "personalized medicine".

In the present study, we aimed to establish an *in vitro* 3D hOBs/hOCs co-culture model requiring a minimal amount of cells, and therefore particularly suitable to apply to primary bone cells that cannot be obtained in a large amount, since harvested from compromised tissue areas such as from jawbone osteonecrotic specimens. In order to establish culture conditions that could be as close as possible to the *in vivo* microenvironment, we used a rotational culture bioreactor as a physiological stimulus to promote cell aggregation and interaction. Importantly, it has been shown that this strategy may be efficiently employed to induce the production of bone-like matrix in the cell aggregates [7] without exogenous scaffolds the use of which may not always be desired since affecting cell metabolism and response to stimuli. The scaffold free system by us developed has the advantage to investigate and monitor the real endogenous properties of the cells. Therefore, besides being one step closer to the *in vivo* microenvironment, culture system here adopted facilitates a fine tuning of the biophysical, biochemical and biomechanical cues, while potentially allowing the monitoring of different parameters and the measurement of soluble factors. Notably, we showed that co-culturing hOBs and osteoclast progenitors (hMCs) in 3D dynamic flow condition (*3D-DyC*) using the RCCS bioreactor led to the formation of cell aggregates that preserved cell viability and exhibited a well defined structure over the entire period of culture. On the contrary, 3D static condition (*3D-C*) is less favorable to produce cell aggregates with a well defined matrix, confirming that the mechanical forces induced by rotational culture are important to promote and maintain the integrity and structure of cellular aggregates, mainly in Xg condition. In fact, the application of modeled gravity (µXg) seems to prevent the osteoblastic cellular component to reach those levels of differentiation showed by cellular aggregates cultured in Xg. This is supported by the expression levels of Osteopontin, Osterix, Runx2 as well as the production of bone mineral matrix at day 21 of culture. This interesting aspect deserves to be investigated in more detail with further experiments

15

to determine the signaling pathways or bioactive molecules leading to the aforementioned phenomena. Regardless the level of osteoblastic maturation, the histochemical and functional analysis confirmed the presence of mature multinucleated hOCs in all the different 3D co-culture models analyzed, without the addition of osteoclastogenic inducers (MCSF/RANKL). Cell aggregates formation without the employment of external osteoclastogenic inducers is relevant since indicates the potency of osteoblastic cellular component and supports the hypothesis of a possible in vivo use of this system to prime endogenous repair phenomena and bone remodeling process in its entirety.

Therefore, as a whole these preliminary data demonstrate the feasibility to establish a 3D dynamic co-culture system keeping the viability and functionality of cellular component (hOBs and hMCs – hOCs) despite a few cells. This condition produced stable cell aggregates exhibiting active matrix remodeling and potentially implantable without scaffold.

After these observations, we aimed to adopt the same conditions to recreate an *in vitro* "oral bone microenvironment" with hOBs from jawbone necrotic area. To the best of our knowledge, an experimental model with this specific purpose is still lacking. In this regards, one of the major challenges that must be overcome is the obtainment of vital and expandable cell populations from compromised tissues such as jawbone of patients taking BPs. For this reason, we tried to isolate osteoblasts from alveolar bone specimens of BPs treated patients, harvested from either boundary bone during surgical treatment of MRONJ lesion or during teeth extraction (hnOBs). Despite the extremely poor quality of the biological specimens, demonstrated by the relatively high incidence of sample contamination or insufficient cell growth (see Table 1), we showed that it is possible to obtain a sufficient number of primary hnOBs able to form an aggregate with hMCs. We hypothesize that optimization of the culture conditions could help to further improve the isolation of hnOBs from the bone chips, in terms of cell number and growth potential. Nevertheless, we confirmed by immunocytochemical analysis that hnOBs prior and after 3D co-culture condition maintain the properties of osteogenic lineage ability producing a typical bone matrix protein such as OPN and mineral matrix.

Our findings, together with previous reports, evidenced the need for deepened studies on local tissue primary cells from patients treated with antiresorptive agents, such as BPs, to determine each cell type specific role in MRONJ onset and development. Pathophysiology of MRONJ is still not fully understood and only few clinical studies have addressed the influence of antiresorptive agents on the cellular mechanisms involved in bone tissue healing/lack of healing in the human oral cavity [30, 24]. Intravenous administration of a single dose of BPs leads on the other hand to rapid accumulation of drug in bone tissue, approximately 60% in 1 hour [22]. Once incorporated into the

bone, BPs are liberated again only when the bone is resorbed, ideally never again, due to the compromised bone turnover [23]. Although length of exposure seems to be a very important risk factor for MRONJ development, early cases were reported also after few doses [3, 2]. Barasch and coworkers showed that the risk for development of MRONJ begins within 2 years of treatment, for both cancer and noncancer patients, showing that even the less potent BPs are linked to MRONJ after a relatively brief treatment period [2].

Considering clinical conditions of patients involved in this study, limitations are the small group of patients, different indications for treatment with antiresorptive agents, different ways of administration (oral and I.V.), and the fact that specimen were taken from different mandible sites during different surgical procedures. Another confounding factor is the large number of other medicines taken by such patients. Generally the risk for developing MRONJ after oral treatment has to be carefully considered for patients with osteoporosis or oncologic diseases and severely compromised tissues. However, although our results must be cautiously interpreted, they are suggestive of possible cell-based tissue engineering approach when associated with surgical procedures for treatment or prevention of MRONJ. To confirm our evidence, further studies with a large sample size are urgently needed even if it is reasonable to think that our data will eventually lead to the in vitro development of smart cell-based constructs with regenerative properties, and therefore potentially able to trigger and promote tissue repair once implanted in the site of the oral defect.

5. Conclusions

In conclusion, we demonstrated the feasibility of a 3D co-culture system with limited amounts of cells preserving viability and functionality of bone cellular components and generating bone-like aggregates also by using cells from jawbone compromised areas. The approach here described will allow to develop in the future a platform useful both to study the molecular mechanisms sustaining the osteonecrosis and test drugs potentially able to revert the aberrant phenotype of pathological OBs. Nonetheless, depending on the cell populations chosen for the co-culture system, such a tool could be exploited not only for diseases affecting the alveolar bone but also other tissues of the oral cavity, such as the jaw muscles or the temporomandibular joint.

17

Conflict of interest statement

The authors declare no conflict of interest.

Acknowledgments

18

References

[1] A. Albanese A, M.E. Licata, B. Polizzi, G. Campisi, Platelet-rich plasma (PRP) in dental and oral surgery: from the wound healing to bone regeneration, Immun. Ageing 10 (2013) 23.

[2] A. Bamias, E. Kastritis, C. Bamia, L.A. Moulopoulos, I. Melakopoulos, G. Bozas, et al., Osteonecrosis of the jaw in cancer after treatment with bisphosphonates: incidence and risk factors, J. Clinical Oncol. 23 (2005) 8580-8587.

[3] A. Barasch, J. Cunha-Cruz, F.A. Curro, P. Hujoel, A.H. Sung, D. Vena, et al., Risk factors for osteonecrosis of the jaws: a case-control study from the CONDOR dental PBRN, J. Dental Res. 90 (2011) 439-444.

[4] P. Barba-Recreo, J.L. Del Castillo Pardo de Vera, T. Georgiev-Hristov, E. Ruiz Bravo-Burguillos, A. Abarrategi, M. Burgueño, et al., Adipose-derived stem cells and platelet-rich plasma for preventive treatment of bisphosphonate-related osteonecrosis of the jaw in a murine model, J. Craniofac. Surg. 43 (2015) 1161-1168.

[5] V. Bloemen, T. Schoenmaker, T.J. de Vries, V. Everts, Direct cell-cell contact between periodontal ligament fibroblasts and osteoclast precursors synergistically increases the expression of genes related to osteoclastogenesis, J. Cell. Physiol. 222 (2009) 565-573.

[6] C. Cardemil, P. Thomsen, C.L. Wexell, Jaw Bone Samples From Bisphosphonate-Treated Patients: A Pilot Cohort Study, Clin. Implant. Dent. Relat. Res. (2015) doi: 10.1111/cid.12307

[7] M.S. Clarke, A. Sundaresan, C.R. Vanderburg, M.G. Banigan, N.R. Pellis, A three-dimensional tissue culture model of bone formation utilizing rotational co-culture of human adult osteoblasts and osteoclasts, Acta Biomater. 9 (2013) 7908-7916.

[8] V.N. Devaki, K. Balu, S.B. Ramesh, R.J. Arvind, P. Venkatesan, Pre-prosthetic surgery: mandible, J. Pharm. Bioallied. Sci. 4 (2012) S414-6.

[9] A.L. Gamblin, A. Renaud, C. Charrier, P. Hulin, G. Louarn, D. Heymann, V. Trichet, P. Layrolle, Osteoblastic and osteoclastic differentiation of human mesenchymal stem cells and monocytes in a miniaturized three-dimensional culture with mineral granules, Acta Biomater. 10 (2014) 5139-5147.

19

[10] M. Gonzálvez-García, F. Rodríguez-Lozano, V. Villanueva, D. Segarra-Fenoll, M.A. Rodríguez-González, R. Oñate-Sánchez, et al., Cell therapy in bisphosphonate-related osteonecrosis of the jaw, J. Craniofac. Surg. 24 (2013) e226-e228.

[11] M. Halai, A. Ker, R.D. Meek, D. Nadeem, T. Sjostrom, B. Su, et al., Scanning electron microscopical observation of an osteoblast/osteoclast co-culture on micropatterned orthopaedic ceramics, J. Tissue Eng. 5 (2014) 1-10.

[12] R.S. Hayden, K.P. Quinn, C.A. Alonzo, I. Georgakoudi, D.L. Kaplan, Quantitative characterization of mineralized silk film remodeling during long-term osteoblast-osteoclast co-culture, Biomaterials 35 (2014) 3794-3802.

[13] S. Heinemann, C. Heinemann, S. Wenisch, V. Alt, H. Worch, T. Hanke, Calcium phosphate phases integrated in silica/collagen nanocomposite xerogels enhance the bioactivity and ultimately manipulate the osteoblast/osteoclast ratio in a human co-culture model, Acta Biomater. 9 (2013) 4878-4888.

[14] C. Heinemann, S. Heinemann, H. Worch, T. Hanke, Development of an osteoblast/osteoclast co-culture derived by human bone marrow stromal cells and human monocytes for biomaterials testing, Eur. Cell. Mater. 21 (2011) 80-93.

[15] Y.F. Huang, C.T. Chang, C.H. Muo, C.H. Tsai, Y.F. Shen, et al., Impact of bisphosphonate-related osteonecrosis of the jaw on osteoporotic patients after dental extraction: a population-based cohort study, PLoS One 10 (2015) e0120756.

[16] C. Jacome-Galarza, S.K. Lee, J.A. Lorenzo, H.L. Aguila, Identification, characterization, and isolation of a common progenitor for osteoclasts, macrophages, and dendritic cells from murine bone marrow and periphery, J. Bone Miner. Res. 28 (2013) 1203-1213.

[17] G.L. Jones, A. Motta, M.J. Marshall, A.J. El Haj, S.H. Cartmell, Osteoblast: Osteoclast co-cultures on silk fibroin, chitosan and PLLA films, Biomaterials 30 (2009) 5376-5384.

[18] H. Kaji, G. Camci-Unal, R. Langer, A. Khademhosseini, Engineering systems for the generation of patterned co-cultures for controlling cell-cell interactions ., Biochim. Biophys. Acta 1810 (2011) 239-250.

[19] E. Knight, S. Przyborski, Advances in 3D cell culture technologies enabling tissue-like structures to be created in vitro, J. Anat. 2014 Nov 20. doi: 10.1111/joa.12257.

20

[20] J. Kuttenberger, E. Polska, B.M. Schaefer, A novel three-dimensional bone chip organ culture, Clin. Oral Investig. 17 (2013) 1547-1555.

[21] G. Li, P. Wu, Y. Xu, Y. Yu, L. Sun, L. Zhu, et al., The effect of Lipoxin A4 on the interaction between macrophage and osteoblast: possible role in the treatment of aseptic loosening, BMC Musculoskelet. Disord. 10 (2009) 57-68.

[22] J.H. Lin, I.W. Chen, F.A. deLuna, On the absorption of alendronate in rats, J. Pharm. Sciences 83 (1994) 1741-1746.

[23] J.H. Lin, Bisphosphonates: a review of their pharmacokinetic properties, Bone 18 (1996) 75-85.

[24] S. Otto, C. Schreyer, S. Hafner, G. Mast, M. Ehrenfeld, S. Stürzenbaum, et al., Bisphosphonate-related osteonecrosis of the jaws – characteristics, risk factors, clinical features, localization and impact on oncological treatment, J. Craniomaxillofac. Surg. 40 (2012) 303-309.

[25] M. Nishi, R. Matsumoto, J. Dong, T. Uemura, Regeneration of bone tissue in a controlled *in vitro* environment with a Rotating Wall Vessel Bioreactor, Nano Biomedicine 3 (2011) 267-274.

[26] A. Papadimitropoulos, A. Scherberich, S. Güven, N. Theilgaard, H.J.A. Crooijmans, F. Santini, A 3D in vitro bone organ model using human progenitor cells, Eur. Cell. Mater. 21 (2011) 445-458.

[27] R. Piva, L. Penolazzi, E. Lambertini, S. Giordano, R. Gambari, Induction of apoptosis of human primary osteoclasts treated with a transcription factor decoy mimicking a promoter region of estrogen receptor alpha, Apoptosis 10 (2005) 1079-1094.

[28] A.A. Reszka, G.A. Rodan, Bisphosphonate mechanism of action, Curr. Rheumatol. Rep. 5 (2003) 65-74.

[29] S. Rosini, S. Rosini, I. Bertoldi, B. Frediani, Understanding bisphosphonates and osteonecrosis of the jaw: uses and risks, Eur. Rev. Med. Pharmacol. Sci. 19 (2015) 3309-3317.

[30] S.L. Ruggiero, T.B. Dodson, J. Fantasia, R. Goodday, T. Aghaloo, B. Mehrotra, et al., American Association of Oral and Maxillofacial Surgeons position paper on medication-related osteonecrosis of the jaw--2014 update, J. Oral Maxillofac. Surg. 72 (2014) 1938-1956.

[31] F. Saad, J.E. Brown, C. Van Poznak, T. Ibrahim, S.M. Stemmer, A.T. Stopeck, Incidence, risk factors, and outcomes of osteonecrosis of the jaw: integrated analysis from three blinded active-

controlled phase III trials in cancer patients with bone metastases, Ann. Oncol. 23 (2012) 1341-1347.

[32] H. Sekine, T. Shimizu, K. Sakaguchi, I. Dobashi, M. Wada, M. Yamato, In vitro fabrication of functional three-dimensional tissues with perfusable blood vessels, Nat. Commun. 4 (2013) 1399.

[33] N.A Sims, T.J. Martin, Coupling the activities of bone formation and resorption: a multitude of signals within the basic multicellular unit, Bonekey Rep. (2014) Jan 8;3:481. doi: 10.1038/bonekey.2013.215. eCollection 2014.

[34] E. Torreggiani, C. Bianchini, L. Penolazzi, E. Lambertini, R. Vecchiatini, A. Canella, et al., Osteogenic potential of cells derived from nasal septum, Rhinology, 49 (2011)148-154.

[35] F. Tortelli, N. Pujic, Y. Liu, N. Laroche, L. Vico, R. Cancedda, Osteoblast and osteoclast differentiation in an in vitro three-dimensional model of bone , Tissue Eng. Part A. 15 2009 2373-2383.

[36] R. Vecchiatini, L. Penolazzi, E. Lambertini, M. Angelozzi, C. Morganti, S. Mazzitelli, et al., Effect of dynamic three-dimensional culture on osteogenic potential of human periodontal ligament-derived mesenchymal stem cells entrapped in alginate microbeads, J. Periodontal. Res. 50 (2015) 544-553.

[37] M. Widbiller, S.R. Lindner, W. Buchalla, A. Eidt, K.A. Hiller, G. Schmalz, et al., Three-dimensional culture of dental pulp stem cells in direct contact to tricalcium silicate cements. Clin Oral Invest (2015) doi 10.1007/s00784-015-1515-3.

[38] M. Zhang, B. Huang, The multi-differentiation potential of peripheral blood mononuclear cells, Stem. Cell. Res. Ther. 3 (2012) 48-58.

Figure Legends

Fig. 1. Isolation and characterization of human osteoblasts and monocytes for the co-culture system. (A) Human primary osteoblasts (hOBs) were isolated from bone specimens and characterized in terms of morphology, ALP activity and expression of OPN and Runx2 by immunocytochemistry. hOBs were assayed for mineralization capacity by Alizarin Red S (ARS) staining after culture in osteogenic medium (ost) for 21 days (ctr = cells cultured in basal medium). (B) Human primary monocytes (hMCs) were isolated from peripheral blood and characterized in terms of morphology and CD14 expression by FACS analysis (CD14 positive cells ≥95%). The ability of hMCs to differentiate into mature osteoclasts (hOCs) was confirmed in terms of TRAP-positivity, MMP9 and Cathepsin K expression after stimulation with MCSF (25ng/mL) and RANKL (30 ng/mL) for 7 days. Bars: 250 μm. The pit formation ability of hOCs is also reported. Bars: 20 μm.

Fig. 2. Experimental set-up of *in vitro* hOBs/hMCs co-culture system. In order to establish a hOBs/hMCs co-culture system, hOBs were plated and after 7 days hMCs were seeded on the apical side of culture plate inserts (day 0). At day 7 of co-culture, the presence of differentiated hOCs (indicated by arrows) was evaluated by TRAP assay (a, b) and Cathepsin K expression (g). The analysis was also performed after stimulation with MCSF/RANKL (c, d, h: positive control) and in the absence of hOBs (e, f, i: negative control). Bars: 50 μm. Afterwards, osteogenic differentiation of hOBs was induced by replacing the basal medium with osteogenic medium. At day 21 of co-culture, the presence of osteogenic markers was assessed by immunostaining for OPN, OSX, Runx2, ALP activity and ARS staining for mineralized bone matrix. Bars: 20 μm.

Fig. 3. Establishment of three-dimensional (3D) hOBs/hMCs co-culture models. (A) After expansion in monolayer, hOBs were trypsinized and seeded with hMCs (day 0) in agarose-coated wells (3D static condition = *3D-C*) or inoculated in HARV culture vessels with the dynamic RCCS bioreactor culture system (3D dynamic condition = *3D-DyC*). All the tested experimental conditions are reported in the inset as cell number and ratio (hOBs/hMCs), exposure to differentiating agents (MCSF/RANKL), rotation rate (rpm) and presence or not of controlled microgravity (μXg – modelled microgravity), days of co-culture. (B) At day 7 of co-culture, the presence of mature hOCs was evaluated by TRAP assay in *3D-C* and *3D-DyC* condition. Higher magnification fields are reported. Bars: 50 μm. TRAP activity was quantified by densitometric analysis using ImageJ software and expressed as percentage of positive area (5 sections per sample, n=3). Data are presented as means ±sem. Statistical analysis was performed: *= p≤0.0001.

23

Fig. 4. Morphological features and viability of *3D-C* and *3D-DyC* aggregates generated at day 7 and day 21 of co-culture. It is appreciable by haematoxylin staining that only *3D-DyC* constructs at day 21 displayed a noticeable cellular organization in three different cell layers: an outer region (arrows) surrounding the construct, an intermediate region with a trabecular-like structure and an inner region. Representative Calcein-AM fluorescence images of live cells and Propidium iodide (PI) fluorescence images of dead cells at day 21 of co-culture have been reported. Bars: 50 μm.

Fig. 5. Histochemical characterization of *3D-C* and *3D-DyC* aggregates, cultured under Modeled Microgravity (μXg) or Ground Based dynamic culture (Xg). (A) The aggregates were characterized to determine hOCs activity by TRAP assay and Cathepsin K. Higher magnification fields are indicated by the boxed areas and reported in the flanking columns. Bars: 50 μm. Multinucleated mature hOCs are arrowed. (B) The aggregates were characterized to determine hOBs activity by the analysis of OPN, OSX, Runx2 expression levels together with ARS staining. Higher magnification fields are indicated by the boxed areas and reported in the flanking columns. Bars: 50 μm.
All microphotographs illustrate representative results of the different experimental conditions. The stainings were quantified by ImageJ software and expressed as % of positive area (mean value ± sem, 5 sections per sample, n=3). ND: not detectable. *p<0.05 vs 3D-C.

Fig. 6. Isolation and characterization of human primary osteoblasts obtained from alveolar bone samples of patients taking BPs (hnOBs). (A) Sample from patient with a potential diagnosis of MRONJ was harvested (abc) and characterized in term of cell morphology, expression of OPN and Runx2 by immunocytochemistry. hnOBs were also assayed for mineralization capacity by ARS staining after culture in osteogenic medium (ost) for 21 days (ctr = cells cultured in basal medium). (B) Viability and histochemical characterization of hnOBn/hMC *3D-DyC* aggregates generated after 21 days in Xg condition (4rpm). Fluorescence photomicrograph is representative merged image and shows the presence of green fluorescence (Calcein-AM)-labelled live cells and the absence of red fluorescence (PI)-labelled dead cells. Analysis of the histological sections confirmed the presence of TRAP positive multinucleated osteoclasts. OPN positive staining localized the presence of functional osteoblasts. ARS staining is also reported. TRAP activity, ARS staining and OPN levels were quantified by ImageJ software and expressed as % of positive area (mean value ± sem, 5 sections per sample, n=2). Bars: 50 μm.
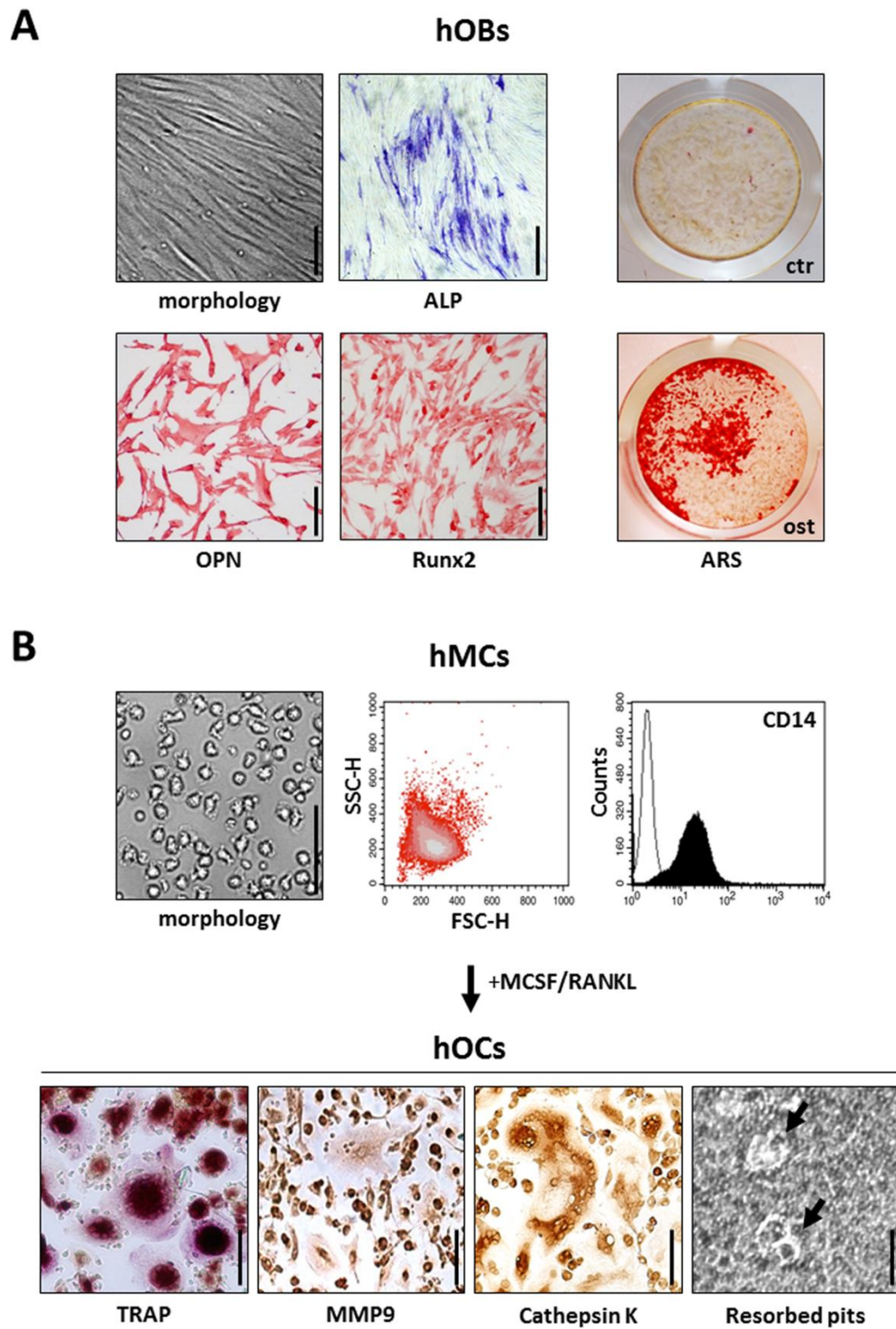
24

Figure 1

25

Figure 2
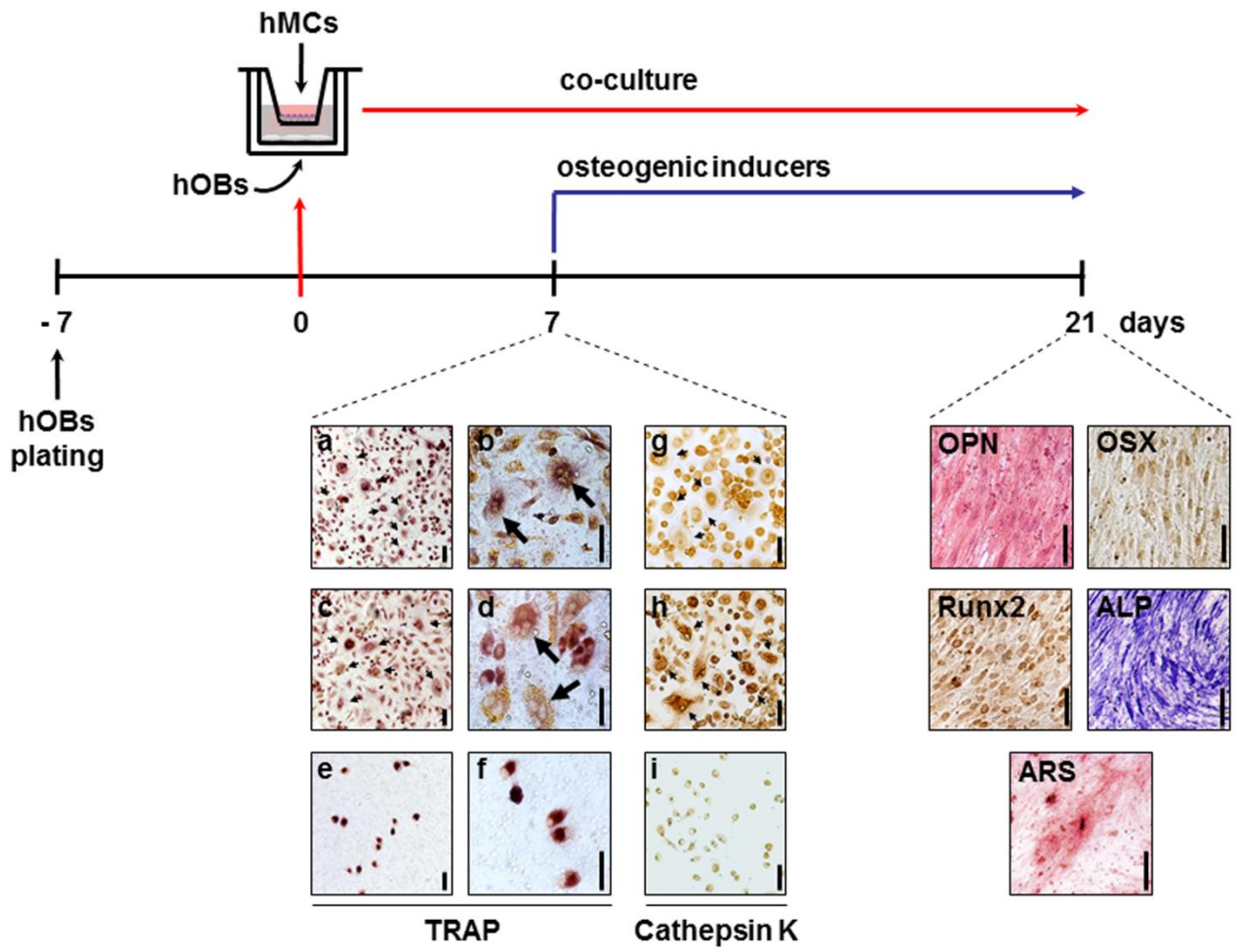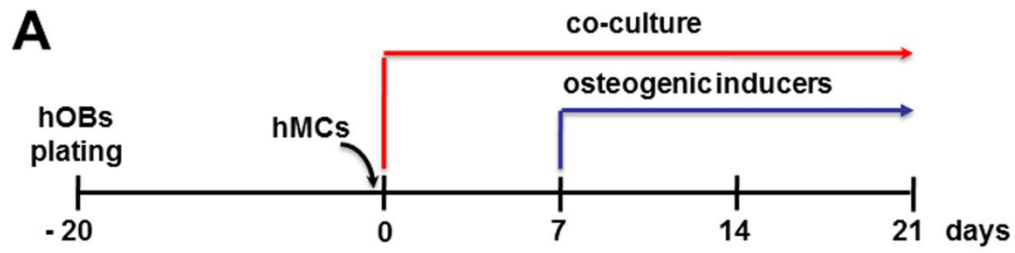
A

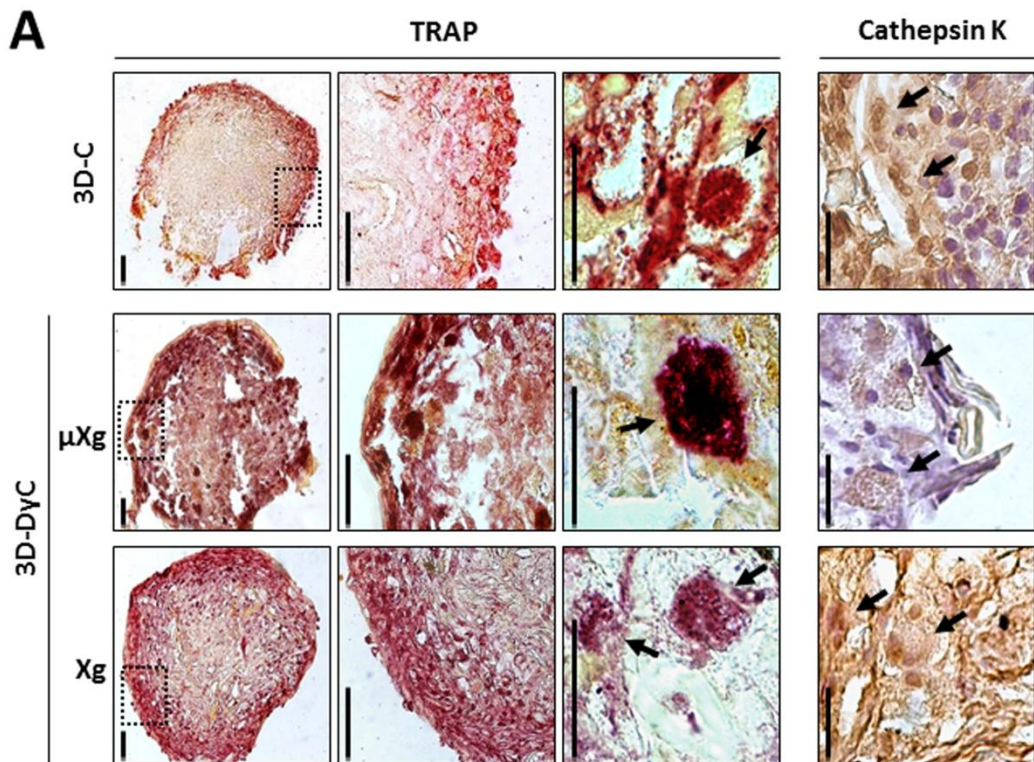| Co-culture system	Cell number	hMCs/hOBs ratio	MCSF/ RANKL	Rpm	Days
3D-C					
	3×10^6	1:2	-	-	7
	3×10^6	1:2	-	-	21
	3×10^6	1:3	-	-	21
	2×10^6	1:2	-	-	21
	2×10^6	1:2	+	-	21
3D-DyC					
	3×10^6	1:2	-	14 (µXg)	7
	3×10^6	1:2	+	14 (µXg)	21
	3×10^6	1:2	-	14 (µXg)	21
	3×10^6	1:3	-	14 (µXg)	21
	2×10^6	1:2	-	14 (µXg)	21
	2×10^6	1:2	-	4 (Xg)	21
	3×10^6	1:2	-	4 (Xg)	21

B
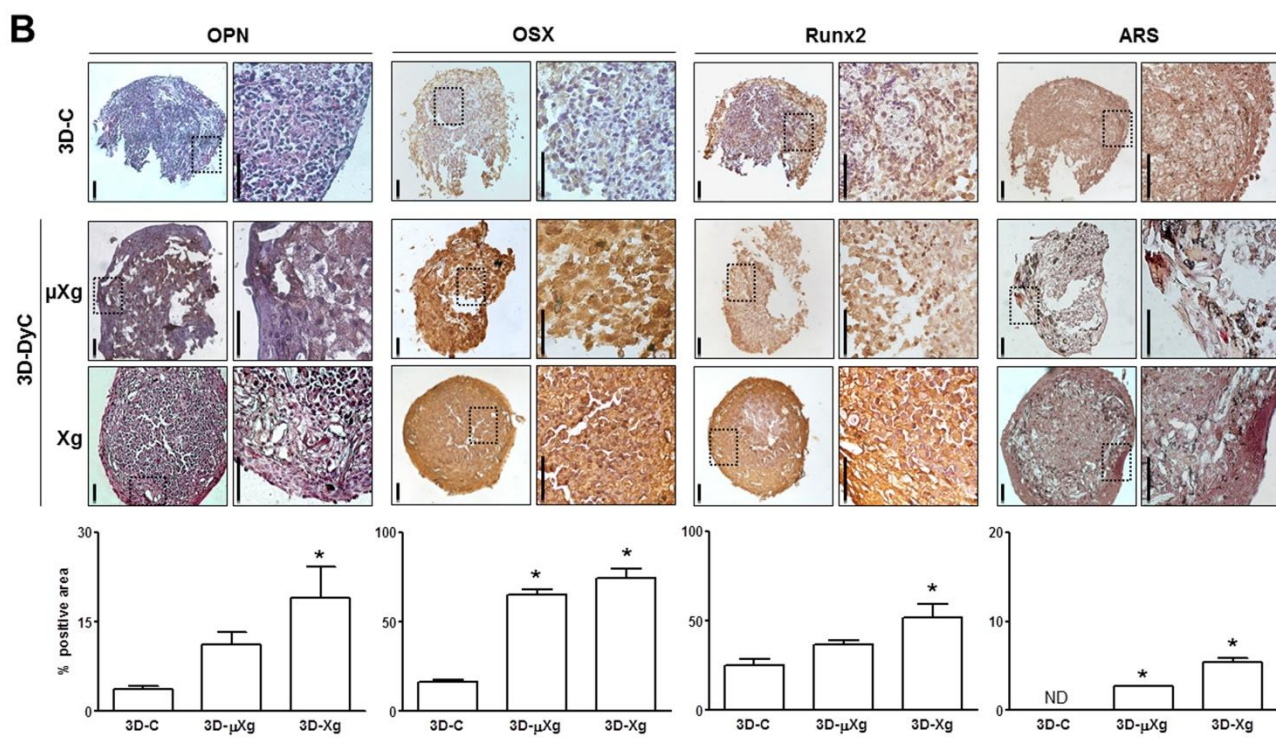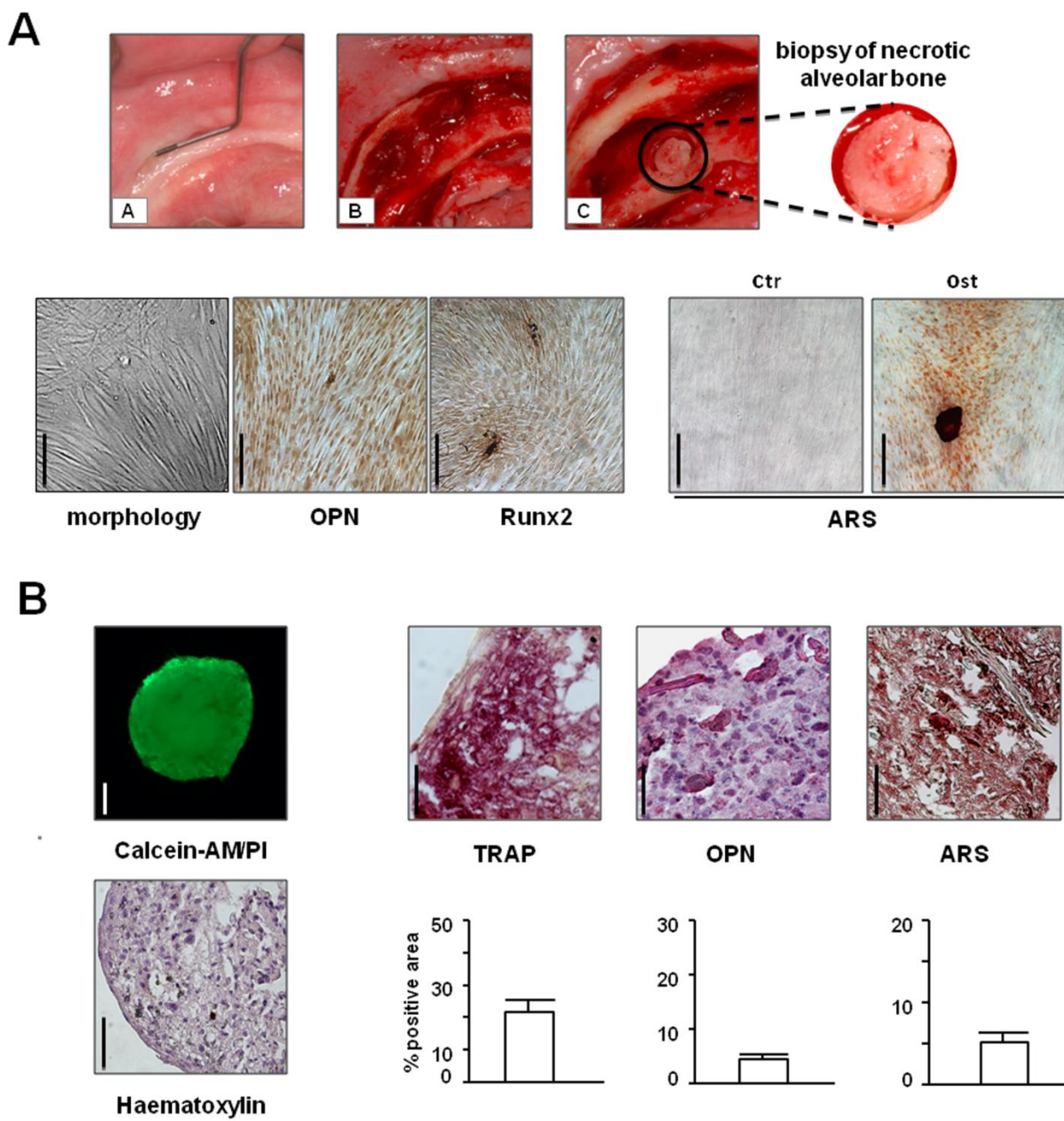

Figure 3

Figure 4

A

29

Figure 5

Figure 6

31
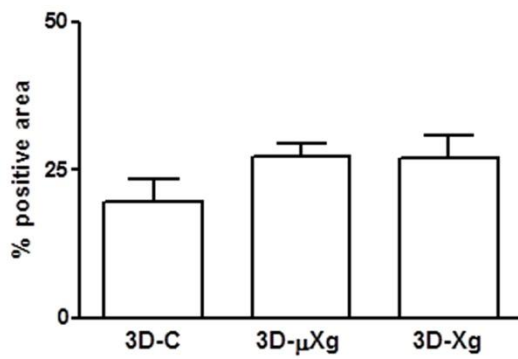
Table 1. Clinical parameters of the patients included in the study

Sample	Age	Gender	BP	Treatment indication	Drug Administration	Therapy duration	Co-morbidities	Indication for referral	Jaw	ONJ onset (within 12 months)	Cell attachment	Cell proliferation
1	73	F	ALNa	osteoporosis	oral	10 yrs	none	surgical extraction	manda	none	+	-
2	80	F	ZOLa	Multiple myeloma	i.v.a	24 months	none	surgical extraction	manda	none	+	contaminated
3	70	F	ALNa	osteoporosis	Oral	5 yrs	Takotsubo Syndrome	surgical extraction	manda	none	-	-
4	64	F	ALNa	osteoporosis	Oral	5 yrs	Type I diabetes	surgical extraction	manda	none	+	contaminated
5	70	F	ZOLa CLODRa	Multiple myeloma	i.v.a i.m.a	4 months 6 months	Osteoporosis Type I diabetes Former smoker	surgical treatment of MRONJ	manda	Complete healing within 2 months	+	+
6	67	F	ALNa	osteoporosis	Oral	7yrs	Type I diabetes smoker	surgical extraction	manda	none	+	+

a*ALN: alendronate; ZOL: zoledronate; CLODR:clodronate; i.v.: intravenous; i.m.: intramuscular; mand: mandible*

32